Orbital
The electronic journal of chemistry

the electronic journal of chemistry

Full Paper | http://dx.doi.org/10.17807/orbital.v15i4.19352

Optimization of the Removal of Hexavalent Chromium Cr(VI) from Aqueous Solution by *Moringa oleifera* Bark-Derived Activated Carbon (MOBAC) Using Response Surface Methodology (RSM)

Evon P. Acut* [a], Nova Fe A. Anorico [a], and Dharel P. Acut [b,c]

This study investigated the removal of hexavalent chromium Cr(VI) ions in an aqueous solution using *Moringa oleifera* bark-derived activated carbon (MOBAC). The adsorption removal of Cr(VI) was systematically investigated as a function of four experimental factors: pH (1-5), contact time (10-90 min), adsorbent dosage (0.020-0.100 g L^{-1}), and temperature (25-45°C) by following a statistical experimental design. A response surface methodology (RSM)-based central composite experimental design was used to establish an empirical model that assessed factors' effects on Cr(VI) ions adsorptive removal. The model was verified and validated and used to predict optimal adsorption removal of Cr(VI) from aqueous solutions. At optimized conditions, 99.612 % of 1.5 mg L^{-1} Cr(VI) ions are removed from the aqueous solution. These optimum condition values include a pH of 2.1, contact time of 62.72 min, adsorbent dosage of 0.065 g L^{-1}, and temperature of 39.8°C. The adsorptive mechanism was assessed by conducting isotherm and kinetic studies. The adsorption process of Cr(VI) ions by MOBAC is described by Langmuir isotherm, indicating monolayer adsorption, and the reaction kinetics is described by pseudo-second order kinetics model. The Langmuir monolayer adsorption capacity of Cr(VI) adsorption on MOBAC was found to be 4.577 mg g^{-1} for Cr(VI) ions. The findings support the use of MOBAC in the removal of Cr(VI) ions from aqueous systems.

Graphical abstract

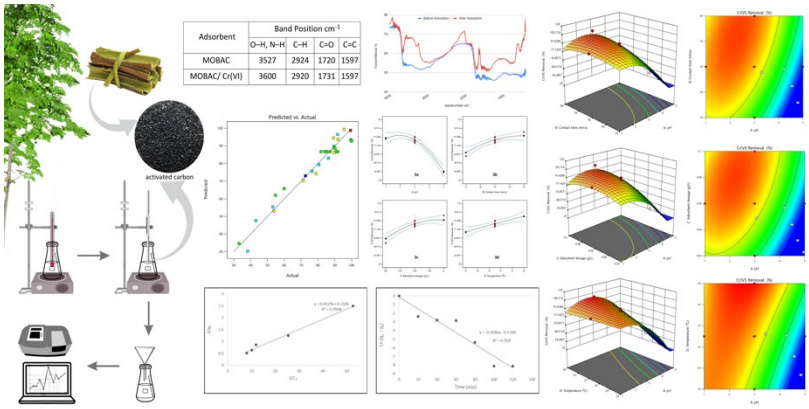

Keywords

Activated carbon
Adsorption isotherm
Adsorption kinetics
Hexavalent chromium removal
Response surface methodology

Article history

Received 03 Sep 2023
Revised 12 Nov 2023
Accepted 14 Nov 2023
Available online 29 Dec 2023

Handling Editor: Grégoire Demets

[a] Department of Chemistry, College of Science and Mathematics, University of Science and Technology in Southern Philippines, Cagayan de Oro City, Misamis Oriental 9000 Philippines.[b] College of Arts and Sciences, Colegio de San Antonio de Padua, Danao City, Cebu 6004, Philippines.[c] National Research Council of the Philippines, Taguig City, Metro Manila 1631 Philippines. *Corresponding author. E-mail: **acut.evonp@gmail.com**

1. Introduction

Water quality is crucial for human health, social and economic development, and ecosystem sustainability. However, as industries and population increase, natural environments deteriorate, leading to pollution of water resources. Organic and inorganic pollutants, including heavy metals, are discharged from activities like industrial production, mining, and agriculture into natural water sources [1,2]. These pollutants pose a significant threat to humans and other living species [3]. Chang [4] and Babula et al. [5] discuss the harmful effects of heavy metals, with most becoming toxic at concentrations above a threshold. Hexavalent chromium Cr(VI) ion is particularly concerning due to its rapid transport across cell membranes and reduction to Cr(III) form. This results in insoluble complexes that are difficult to eject by the affected organism [6-9].

Chromium (VI)-containing wastewater is primarily discharged from industries such as electroplating, tanneries, mud drilling, textile industries, and mining. Depending on the pH of the solution, Cr (VI) can exist as divalent chromate (CrO_4^{2-}) ions, dichromate ($Cr_2O_7^{2-}$) ions, or hydrogen chromate ($HCrO_4^-$) ions. Because these divalent oxyanions are highly soluble in water and poorly adsorbed by soil and organic matter, they are mobile in groundwater. The World Health Organization (WHO) sets maximum limits for Cr(VI) in surface, industrial, and drinking water (water for consumption) of 0.10, 0.25, and 0.05 mg/L, respectively [10,11]. Wastewater from industries must be treated to keep Cr(VI) concentrations within recommended limits.

Various methods, including ion exchange, precipitation, electrocoagulation, biological methods, coagulation, and membrane separation, are used to remove Cr(VI) from wastewater. However, these techniques have drawbacks like toxic by-products, high energy requirements, incomplete removal, low selectivity, and high operational costs. Studies on the removal of heavy metals from wastewater using affordable and environmentally friendly methods, like adsorption, have received a considerable attention recently. Due to its simplicity, economic effectiveness, environmental friendliness, and ease of operation, adsorption exhibits good potential as a substitute treatment for the removal of Cr(VI) ions [12-16].

By reducing pollution and using nonrenewable resources to treat wastewater, green chemistry focuses on environmental sustainability. In recent years, biosorption, a sustainable option utilizing biomass sources, has demonstrated to be an effective method for addressing pollution and encouraging an eco-friendly approach to wastewater treatment [17,18]. Researchers have tested biosorbents made from agro-wastes like sugarcane bagasse, tea waste, rice husk, peanut shells, corn cob, cactus leaves, watermelon rind, and orange peel for wastewater treatment. While these biosorbents are cheap, efficient, and readily available, their metal sequestration capacity is poor. Techniques like cross-linking, chemical modification, and activation can increase this capacity for highly efficient adsorption [19,20]. In fact, Anastopoulos et al. [21] reported that agro-industrial waste without prior treatment could cause problems with chemical and biological oxygen demand, resulting in environmental pollution and harmful effects on human and animal health [22].

Activated carbons (ACs), which are made from a variety of raw materials, are widely used adsorbents for wastewater treatment and emissions treatment. When made from waste materials, they are both cost-effective and environmentally friendly [23]. The production of activated carbons has been influenced by environmental awareness, with a focus on cheap, plentiful materials like agricultural by-products [24]. These substances ought to yield high-quality activated carbon, have appropriate surface functional groups, and have little effect on the environment.

The production of AC from biomass material for the removal of Cr(VI) ions in an aqueous solution has been prepared and studied. In recent years, numerous studies have been conducted in order to obtain ACs from a variety of low-cost materials. Some of these materials include hazelnut shell [25-27]; apple shells [28]; bamboo bark [29]; Sargassum [30]; Daniellia oliveri stem bark [31], and Moringa oleifera leaves and bark [32,33]. High carbon agricultural waste materials produce AC and contain lignocellulosic compounds and polar functional groups, making them potential sources for carbon production [34,35]. By providing an electron pair to complex the metal ions in solution, these functional groups have the ability to bind heavy metals [36]. All these studies have found that the produced ACs have comparable and higher adsorption capacities compared to commercially available varieties.

In this study, *Moringa oleifera* bark were used as the precursor material for the production of activated carbon. The bark was chemically activated using phosphoric acid and then carbonized. The aim of this study is to prepare activated carbon from *Moringa oleifera* bark and investigate its maximum percent removal of Cr(VI) in aqueous solution. Specifically, this study is guided with the following specific objectives, to wit: (1) determine the characteristic functional groups present on the Moringa oleifera bark-derived activated carbon (MOBAC) involved in the adsorption process; (2) investigate and determine the optimum values for pH, contact time, adsorbent dosage, and temperature that will yield the maximum level of adsorption of Cr(VI) by MOBAC; (3) determine the optimum percent removal, maximum adsorption capacity of Cr(VI) by MOBAC; (4) identify the correlation of parameters in the adsorption process using response surface modeling; and (5) investigate the adsorption process in terms of adsorption isotherms and adsorption kinetics.

2. Material and Methods

2.1 MOBAC sample preparation

Moringa oleifera bark (MOB) was collected during harvesting and trimming period and placed in a clean, dry sack to prevent contamination. The bark was washed multiple times with distilled water, cut into smaller pieces, sun-dried for three (3) days, and oven-dried at 110°C for seven (7) h. The dried bark was ground and sieved to a 1 mm particle size [37]. Through chemical activation and carbonization, the biomass from the bark was converted into activated carbon [38]. To ensure that the reagents were completely adsorbed onto the raw material, the bark was combined with the phosphoric acid at a 1:2 impregnation ratio (weight of MOB: weight of phosphoric acid), stirred continuously, and soaked for 24 h at 25°C. The mixture was dried for 1.5 h at 110°C before being transferred to a sealed container. For 1 h, the dried mixture was carbonized in a furnace at 400°C. The produced MOBAC was repeatedly washed with deionized water until the solution

was neutral. The washed activated carbon was dried in a hot air oven at 110°C for 3 h before being weighed. The prepared materials were kept in a tightly sealed container.

2.2 Cr(VI) ions standard solution preparation

A stock solution of 500 µg/mL Cr(VI) was prepared by dissolving 141.4 mg of potassium dichromate ($K_2Cr_2O_7$) ions in deionized water, and diluting it to the calibration mark of a 100-mL volumetric flask. The working standard solution of Cr (5 µg/mL) were prepared by diluting 1.00 mL of stock Cr solution in 100-mL volumetric flask. The standard calibration solutions (0.3, 0.6, 0.9, 1.2, and 1.5 µg/mL) from (5 µg/mL) working standard Cr solution was put individually in 100-mL volumetric flask and filled to the mark with deionized water. For the pH adjustments, H_2SO_4 and NaOH ions were used. All chemicals utilized in this work were of analytical reagent (AR) grade.

2.3 Adsorption experiments

Thirty (30) batch adsorption experiments were conducted to study the effect of solution pH (1-5), contact time (10-90 min), adsorbent dosage (0.020-0.100 gL^{-1}), and temperature (25-45°C). Each experiment was carried out in 100 mL Cr(VI) ion solution at a known initial concentration of 1.5 µg/mL. The pH adjustments were carried out either by the addition of H_2SO_4 or NaOH ions. The isotherm and kinetic studies were performed by varying the initial concentration and contact time from 0.3 µg/mL to 1.5 µg/mL and from 20 min to 120 min, respectively. The batch isotherm and kinetic experiments were conducted using the optimum condition values (pH 2.1, contact time at 62 min, and temperature at 40°C) obtained from RSM.

2.4 Adsorbent characterization

The functional group of MOBAC was determined using a Fourier Transform Infrared Spectroscopy (FTIR) Spectrophotometer (Shimadzu IR Affinity-1S). The vibrational frequency changes of the functional groups in the adsorbents were determined using the FTIR spectra of chemically activated MOB before and after Cr(VI) ion adsorption. FTIR analysis allows for spectrophotometric observation of the adsorbent surface in the 400-4000 cm^{-1} range and serves as a direct method for identifying functional groups on MOBAC surfaces.

2.5 Analytical Methods

After all kinetic and equilibrium studies, the resulting mixture was filtered using a filter paper (Whatman No.1) and the filtrate was analyzed. The concentrations of Cr(VI) in the solutions derived from all runs were measured spectrophotometrically (Biobase BK-D560 Double Beam Scanning UV/VIS Spectrophotometer) by adding 2.0 mL of 1,5-diphenylcarbazide (DPC) in an acid medium. The 1,5-Diphenylcarbazide solution (DPC) was prepared by dissolving 1 g of 1,5-diphenylcarbazide (DPC) in 200 mL acetone and stored in a bottle. Absorbance was measured at the wavelength λ = 550 nm. The Cr(VI) ions removal efficiency (%) and adsorption capacity (q_e) were calculated according to the following equations:

$$\%\ Removal = \frac{(C_i - C_f)}{C_i} x100 \quad \text{(Eq. 1)}$$

$$q_e = \frac{(C_i - C_f)V}{W} \quad \text{Eq. 2)}$$

where C_i is the initial metal concentration (mg L^{-1}), C_f is the final metal concentration (mg L^{-1}), V is the volume of the metal solution (L) and W is the weight of the activated carbon (g).

A standard RSM design called central composite design (CCD) was employed in this work to study the variables and the response. This method is suitable for fitting a quadratic surface and it helps to optimize the effective parameters with a minimum number of experiments, as well as to analyze the interaction between the parameters. The independent variables utilized in this study were pH of the solution (A), contact time (B), adsorbent dosage (C), and temperature (D). Table 1 shows how these four variables and their respective ranges were chosen based on the literature and preliminary studies.

Table 1. Independent variables and their coded levels for the CCD.

Variables	Code	Units	Coded variable levels				
			-α	-1	0	+1	+α
pH	A		1.0	2.0	3.0	4.0	5.0
Contact time	B	min	10	30	50	70	90
Adsorbent dosage	C	gL^{-1}	0.020	0.040	0.060	0.080	0.100
Temperature	D	ºC	25	30	35	40	45

For each categorical variable, a 23 full factorial central composite design for the four (4) variables, consisting of 14 factorial points, 8 axial points, and 6 replicates at the center points were employed indicating that altogether 30 experiments were required, as calculated from the equation:

$$N = 2^k + 2k + c_p = 2^4 + 2(4) + 6 = 30 \quad \text{(Eq. 3)}$$

where N is the total number of experiments required, k is the number of factors, and c_p is the number of experiments at the center point.

Each independent variable was carried out over the coded levels between -1 and +1 at specific ranges (Table 1). The real values coded +1 are the highest values, while the real values coded with -1 are the lowest. The real values coded with 0 are the control values and the real values coded with +α and - α are the highest and lowest outside values, respectively. The α value was fixed at 2.00 (rotatable).The calculation of real values into coded values are shown in the following equations, where X = α:

$$\text{pH} \quad X_1 = \frac{(pH - 3.0)}{1} \quad \text{(Eq. 4)}$$

$$\text{Contact time} \quad X_2 = \frac{(C_T - 50)}{20} \quad \text{(Eq. 5)}$$

$$\text{Adsorbent dosage} \quad X_3 = \frac{(A_D - 0.060)}{0.020} \quad \text{(Eq. 6)}$$

$$\text{Temperature} \quad X_4 = \frac{(T - 35)}{5} \quad \text{(Eq. 7)}$$

The response is the percent removal of Cr(VI) ions (Y). The response was used to develop an empirical model that

correlated the response to the variables using a second-degree polynomial equation as given by the equation:

$$Y = \beta_o + \sum_{i=1}^{k} \beta_i X_i + \sum_{i=1}^{k} \beta_{ii} X_1^2 + \sum_{i \le i \le j}^{k-1} \beta_{ij} X_i X_j \quad \text{(Eq. 8)}$$

where Y is the predicted response; X_i and X_j are the factors (pH, contact time, adsorbent dosage, and temperature); β_o is the constant coefficient; β_i is the linear coefficient; β_{ii} is the quadratic coefficient; β_{ij} is the interactive coefficients.

The optimization and response surface modelling of the Cr(VI) ion removal efficiency of the MOBAC were done using the statistical software package Design Expert. The significance level of all the polynomial equation terms was analyzed statistically by computing F and p values of 0.05. Three-dimensional surface plots were generated in order to understand the effects of the process variables (pH, contact time, adsorbent dosage, and temperature) on predicting the responses (percent Cr(VI) ion removal). The data were then assessed using the analysis of variance (ANOVA to test the validity of the generated model. The lack-of-fit of the obtained response with the model was established by using the correlation coefficient (R^2). The developed models were assessed by their corresponding F and p-values. Higher F values with lower p values corresponded with the significant models. Following the completion of optimization, the model equation's suitability for predicting the optimal response was validated by comparing the predicted values and the actual values. Adequate precision (AP) were also evaluated to test the model significance and adequacy.

The adsorption mechanism of Cr(VI) ions onto the surface of the MOBAC was described using two (2) well-known isotherm models, namely the Langmuir and Freundlich isotherm models. The Langmuir isotherm model is based on the assumption of monolayer adsorption onto a surface with the equivalent and identical number of localized sites [39]. It also implies that when the monolayer has been covered, no additional adsorption occurs [40]. The Langmuir equation is expressed in linear form:

$$\frac{C_e}{q_e} = \frac{1}{k_L q_m} + \frac{C_e}{q_m} \quad \text{(Eq. 9)}$$

where q_m (mg/g) and k_L (L/mg) represent maximum adsorption capacity and Langmuir constant linked to adsorption energy, respectively. C_e is the equilibrium concentration, and q_e is the equilibrium adsorption capacity.

The Freundlich adsorption isotherm model describes adsorption by heterogeneous surfaces (adsorbent) beyond the first monolayer empirically. It is also assumed that the surfaces' strongest available binding sites are first occupied, and that adsorption increases as the number of available adsorption binding sites increases [41]. The following equation expresses the linear form of the Freundlich isotherm:

$$ln\ q_e = ln\ k_F - \frac{1}{n} \ln C_e \quad \text{(Eq. 10)}$$

where 1/n is described as the adsorption intensity and K_F is related to adsorption capacity (L/mg).

Moreover, adsorption kinetics studies were carried out to describe the rate of Cr(VI) uptake onto the optimized MOBAC, and they provided significant insight into the adsorption mechanism between the adsorbent and the adsorbate. Two kinetic models, pseudo-first and pseudo-second order, are used to determine the adsorption mechanism of Cr(VI) ions. The adsorption of liquid-solid systems based on the solid capacity follows a pseudo-first-order model [42]. Generally, the pseudo-first-order kinetic model is only applicable for the initial stage of the adsorption process and is computed using the linear equation:

$$ln = (q_e - q_t) = lnq_e - k_1 t \quad \text{(Eq. 11)}$$

where q_e (mg/g) represents the amount of Cr(VI) adsorbed on the adsorbent, q_t (mg/g) is the adsorbed Cr(VI) amount on the adsorbent at a certain times *(t)*, and k_1 is known as the 1st order constant.

The pseudo-second-order model predicts the adsorption over a range of different points in time during the adsorption process. The linear equation for pseudo-second-order model is represented as:

$$\frac{t}{q_t} = \frac{1}{k_2 q_e^2} + \frac{1}{q_e} t \quad \text{(Eq. 12)}$$

where k_2 (g/mg min) represents the 2nd order rate constant. At equilibrium, q_e represents the adsorbed amount of the Cr(VI) at certain times (q_t).

3. Results and Discussion

3.1 Adsorbent surface characterization

The surface chemistry of the adsorbent and its effect on the adsorption process is generally investigated using FTIR. The spectra of the adsorbent were measured with wave number ranging from 4000-400 cm^{-1}. The spectra were plotted using the same scale on the transmittance axis for the adsorbent before and after adsorption. The FTIR spectra of MOBAC display number of adsorption bands, indicating the complex nature of the studied adsorbents (Table 2).

Table 2. Fundamentals infrared frequencies of MOBAC before and after adsorption.

	Band Position cm^{-1}			
Adsorbent	O–H, N–H	C–H	C=O	C=C
MOBAC	3527	2924	1720	1597
MOBAC/ Cr(VI)	3600	2920	1731	1597

A wide broadband can be found at 3527 cm^{-1}, related to O–H stretching vibrations or N-H extension vibration [43] of cellulose, pectin, hemicellulose, and lignin components. According to Pérez Marín et al. [44], free hydroxyl groups and bonded OH bands of carboxyl groups were observed as the OH stretching vibrations occurs within a broad range of frequencies. The bands at 2924-2854 cm^{-1} are assigned to the C-H stretching and symmetric C-H bending, respectively. The band around 1720 cm^{-1} corresponds to the carbonyl group in a quinone with strong vibrations from a combination of C=O and C=C [45]. The bands at 1597 cm^{-1} can be attributed to the stretching vibration of C=C in the aromatic rings. The bands at 1419 cm^{-1} are assigned to C-H bending in alkane or alkyl groups. The bands at 1267-1187 cm^{-1} were assigned to C-OH stretching vibrations in the carboxylic, phenolic or lactonic groups indicating the presence of oxygen functional group. The bands at 655-802 cm^{-1} were assigned to the C-C stretching. Due to the presence of such functional groups, MOBAC shows acidic nature. At lower pH, the functionality of these groups is not changed but at higher pH, these groups begin to neutralize changing their activity and binding properties.

Comparing the spectra before and after adsorption of Cr(VI) ions, differences in the position of the absorbance bands appeared. The asymmetrical stretching vibration at 3300 cm^{-1} after adsorption of Cr(VI) ions was significantly distorted suggesting that chemical interactions occurred

between the metal ions and the hydroxyl groups on the adsorbent surface. Observable shifting of bands was depicted on the amine (N-H) band (3527.80-3442.06 cm^{-1}). A shift in position of C=O at 1744 cm^{-1} shifted to 1640 cm^{-1} as the OH was involved in binding Cr(VI) ions. Similarly, the bending modes of aromatics have also shifted, indicative of association with the aromatic rings (Fig. 1).

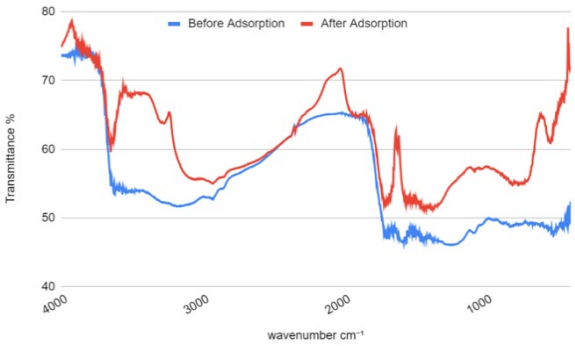

Fig. 1. FTIR result for MOBAC before and after adsorption.

3.2 Model development, validation, and diagnostic analysis

In this study, four factors with full factorial CCD approach were used to investigate and optimize the interactive effects of each process variable (pH, contact time, adsorbent dosage, and temperature) on the adsorption of Cr(VI) ions. A total of 30 batch statistically designed experiments, including six center points, were carried out in triplicates (Table 3). Runs 25-30 at the center point were used to determine the experimental error and the reproducibility of the data. The results from the experiment revealed Cr(VI) ion removal efficiencies that varied from 33.16% to 100%.

The CCD experimental data were analyzed through a sequential model sum of square and summary statistics in order to obtain mathematical empirical models (individual linear, quadratic, cubic and interactive) as listed in Table 4. The results indicated that the linear had higher p-values, compared to the quadratic model for the Cr(VI) metal ions removal. For the linear model, although its p-value was significant for Cr(VI) ion removal, the adjusted R^2 and predicted R^2 values however were found to be low. Hence, the model was not chosen for further analysis. On the other hand, the cubic model was found to be aliased and unsuitable for further developing the experimental data. Towards the end of the study, the quadratic model was selected as the one to effectively describe the effects of process variables (pH, contact time, adsorbent dosage, and temperature) on predicting the responses (Cr(VI) percent removal) using activated carbon since it exhibits low p-values (0.0005) with both high adjusted and predicted R^2 values.

Table 3. Experimental design matrix for the preparation of MOBAC.

Run	Factors				Percent Removal	
	A	B	C	D	Actual	Predicted
	pH	Contact time (min)	MOBAC dosage (g L^{-1})	Temp. (ºC)	(%)	(%)
1	(-1) 2.0	(-1) 30.0	(-1) 0.04	(-1) 30.0	80.53	80.52
2	(+1) 4.0	(-1) 30.0	(-1) 0.04	(-1) 30.0	38.33	29.52
3	(-1) 2.0	(+1) 70.0	(-1) 0.04	(-1) 30.0	86.25	84.22
4	(+1) 4.0	(+1) 70.0	(-1) 0.04	(-1) 30.0	43.15	47.41
5	(-1) 2.0	(-1) 30.0	(+1) 0.08	(-1) 30.0	89.47	91.07
6	(+1) 4.0	(-1) 30.0	(+1) 0.08	(-1) 30.0	53.17	55.16
7	(-1) 2.0	(+1) 70.0	(+1) 0.08	(-1) 30.0	91.66	97.28
8	(+1) 4.0	(+1) 70.0	(+1) 0.08	(-1) 30.0	76.54	75.56
9	(-1) 2.0	(-1) 30.0	(-1) 0.04	(+1) 40.0	89.66	87.49
10	(+1) 4.0	(-1) 30.0	(-1) 0.04	(+1) 40.0	53.89	52.92
11	(-1) 2.0	(+1) 70.0	(-1) 0.04	(+1) 40.0	91.88	94.54
12	(+1) 4.0	(+1) 70.0	(-1) 0.04	(+1) 40.0	78.89	74.14
13	(-1) 2.0	(-1) 30.0	(+1) 0.08	(+1) 40.0	89.30	89.69
14	(+1) 4.0	(-1) 30.0	(+1) 0.08	(+1) 40.0	71.34	70.21
15	(-1) 2.0	(+1) 70.0	(+1) 0.08	(+1) 40.0	95.60	99.25
16	(+1) 4.0	(+1) 70.0	(+1) 0.08	(+1) 40.0	89.29	93.95
17	(-2.00) 1.0	(0) 50.0	(0) 0.06	(0) 35.0	90.18	93.07
18	(+2.00) 5.0	(0) 50.0	(0) 0.06	(0) 35.0	33.16	36.77
19	(0) 3.0	(-2.00) 10.0	(0) 0.06	(0) 35.0	59.53	65.23
20	(0) 3.0	(+2.00) 90.0	(0) 0.06	(0) 35.0	99.47	92.47
21	(0) 3.0	(0) 50.0	(-2.00) 0.02	(0) 35.0	54.83	61.49
22	(0) 3.0	(0) 50.0	(+2.00) 0.10	(0) 35.0	100	91.84
23	(0) 3.0	(0) 50.0	(0) 0.06	(-2.00) 25.0	72.59	72.52
24	(0) 3.0	(0) 50.0	(0) 0.06	(+2.00) 45.0	99.31	97.88
25	(0) 3.0	(0) 50.0	(0) 0.06	(0) 30.0	84.03	86.80
26	(0) 3.0	(0) 50.0	(0) 0.06	(0) 30.0	81.88	86.80
27	(0) 3.0	(0) 50.0	(0) 0.06	(0) 30.0	91.66	86.80
28	(0) 3.0	(0) 50.0	(0) 0.06	(0) 30.0	87.12	86.80
29	(0) 3.0	(0) 50.0	(0) 0.06	(0) 30.0	90.97	86.80
30	(0) 3.0	(0) 50.0	(0) 0.06	(0) 30.0	85.12	86.80

Table 4. Sequential model sum of squares and summary statistics.

Source	Sequential p-value	Lack of Fit p-value	Adjusted R^2	Predicted R^2	
Linear	< 0.0001	0.0168	0.7323	0.6637	
2FI	0.2558	0.0188	0.7572	0.6692	
Quadratic	0.0005	0.1587	0.9138	0.7751	Suggested
Cubic	0.2060	0.1985	0.9418	0.0264	Aliased

3.3 Response surface analysis of Cr(VI) percent removal

According to the sequential model sum of squares, the model was selected based on the highest order polynomials where the additional terms were significant and the models were not aliased. For the percent Cr(VI) ion removal (%), the quadratic model was selected as suggested by the software. From the experimental data, the empirical model was developed by the second-order polynomial equation. This empirical model was based on different process in order to predict the efficiency of Cr(VI) metal ions removal. The empirical model expressed by Equation 13, where the variables take their coded values, represents (Y) as the percent removal, (A) as a function of pH, (B) as a function of contact time , (C) for adsorbent dosage, and (D) for temperature. Variables (AB, AC, and AD) are the interactive effects, whereas A2 and C2 are the quadratic effects. The final empirical formula model for the percent removal (Y) in terms of coded factors is represented by the equation:

$$Y = +86.80 - 13.49A + 6.94B + 7.67C + 6.42D + 3.42AB + 3.65AC + 3.98AD - 6.28A^2 - 2.35C^2 \quad \text{(Eq. 13)}$$

A positive sign in front of the terms indicates synergistic effects, whereas the negative sign indicates an antagonistic effect. The coefficient with one factor represents the effect of the particular factor, while the coefficient with the two factors and those with second–order terms represent the interaction between two factors and the quadratic effect, respectively. The adequacy of the model (Eq. 13) to represent the experimental data was tested by plotting the experimental values against values predicted by the RSM model as shown in Figure 2. The model developed was successful in capturing the relationship between MOB based on the variables and the response because the obtained predicted values were fairly close to the experimental values.

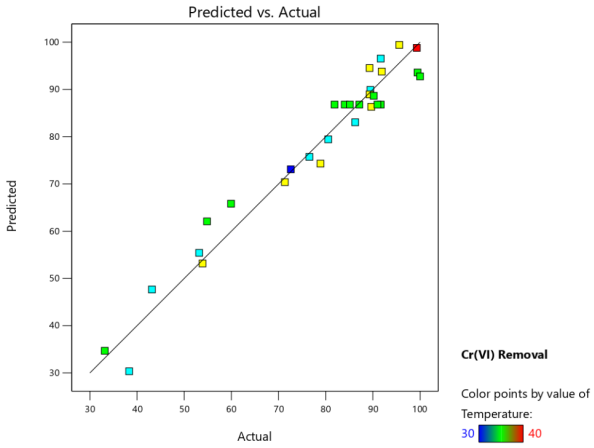

Fig. 2. RSM model experimental values vs. predicted values.

ANOVA was performed to evaluate the acceptability of the model. The results of the second-order response surface model fitting for Cr(VI) percent removal are given in Table 5. The quality of the model developed was evaluated based on the correlation coefficient (R^2) and standard deviation.

Table 5. ANOVA of the quadratic model for Cr(VI) removal efficiency by MOBAC.

Source	Sum of Squares	df	Mean Square	F-value	p-value	Remarks
Model	9848.08	14	703.43	22.97	< 0.0001	significant
A-pH	4368.33	1	4368.33	142.64	< 0.0001	significant
B-Contact time	1157.18	1	1157.18	37.79	< 0.0001	significant
C-Adsorbent dosage	1412.66	1	1412.66	46.13	< 0.0001	significant
D-Temperature	990.61	1	990.61	32.35	< 0.0001	significant
AB	187.07	1	187.07	6.11	0.0259	significant
AC	212.94	1	212.94	6.95	0.0187	significant
AD	253.53	1	253.53	8.28	0.0115	significant
A^2	1082.28	1	1082.28	35.34	< 0.0001	significant
C^2	150.87	1	150.87	4.93	0.0423	significant
Residual	459.37	15	30.62			
Lack of Fit	383.56	10	38.36	2.53	0.1587	not significant
Pure Error	75.81	5	15.16			
Cor Total	10307.45	29				
		Std. Dev. = 5.53 Mean = 78.31 CV % = 7.07			R^2 = 0.9554 Adjusted R^2 = 0.9183 Predicted R^2 = 0.7751 Adeq Precision = 17.6492	

According to Bashir et al. [46], a model is considered to demonstrate a good fit if the coefficient of determination reaches a value of 0.80 and above. The RSM model exhibited satisfactory approximation of the actual Cr(VI) adsorption

removal (%), as demonstrated by the high correlation coefficient (R^2) of 0.9554. In addition, the adjusted correlation coefficient (adj. R^2 = 0.9183) was close to the R^2. An adjusted R^2 is usually preferred over R^2 because the adjusted value only increases upon the addition of statistically significant model terms. The Predicted R^2 of 0.7751 is in reasonable agreement with the Adjusted R^2 of 0.9183 wherein their difference is less than 0.2. Moreover, the standard deviation for the model is 5.53. The closer the R^2 value to unity and the smaller the standard deviation, the better the model will be as it will give a predicted value which is closer to the actual value for the response.

In the present study, ANOVA using the response surface quadratic model was employed to examine the Cr(VI) percent removal of MOBAC. The ANOVA results for quadratic response surface model for Cr(VI) percent removal had an F-value of 22.97 and a corresponding probability greater than F that was less than 0.05. A higher F-value indicates an adequacy of variation about its mean and a p-value (Prob. > F) less than 0.05 indicates the model is significant.

From the ANOVA for the response surface quadratic model for the percent removal (%) of MOBAC, the model F value of 22.97 and Prob. > F as < 0.0001 revealed that the model is significant. In this case A, B, C, D, AB, AC, AD, A2, and C2 were all significant model terms, whereas BC, BD, CD, B2, and D2 were all insignificant for the response. To improve the model's efficiency, the insignificant model terms were excluded from the study. Moreover, the lack-of-fit was also calculated from the experimental error (pure error) and residuals. The lack of fit P-value was greater than 0.05 indicating that lack-of-fit for the mathematical models are insignificant and the quadratic model was valid and significance of the model correlation between the variable process response for the adsorption of Cr(VI).

The adequate precision (AP) measures the ratio between the signal and noise, and determines whether the predicted model can be used to move along the design space [46]. AP values higher than 4 are desirable. In this study, a high AP ratio of 17.6492 was obtained. This indicates that the model can navigate in the space defined by the CCD utilized in this work. The obtained coefficient of variance (CV) value of 7.07 % was below 10%, which meant that the model for Cr(VI) ion removal gave reproducible results. Based on the statistical data obtained, the model presented in this work was efficient and able to predict the Cr(VI) ion removal within the established set of parameters.

3.4 Effects of variables on Cr(VI) adsorption and removal

To investigate the linear effects of changing the levels of a single factor on the response, one-factor effects plots were generated. Figure 3 shows the effects of pH, contact time, adsorbent dosage and temperature on the percent removal of Cr(VI) ions. As depicted in Figure 2, Cr(VI) ion removal was affected by pH, contact time, adsorbent dosage, and temperature. The black circles represent experimental design points, black lines represent modeled prediction, and blue lines represent the least significant difference at a 95% confidence level.

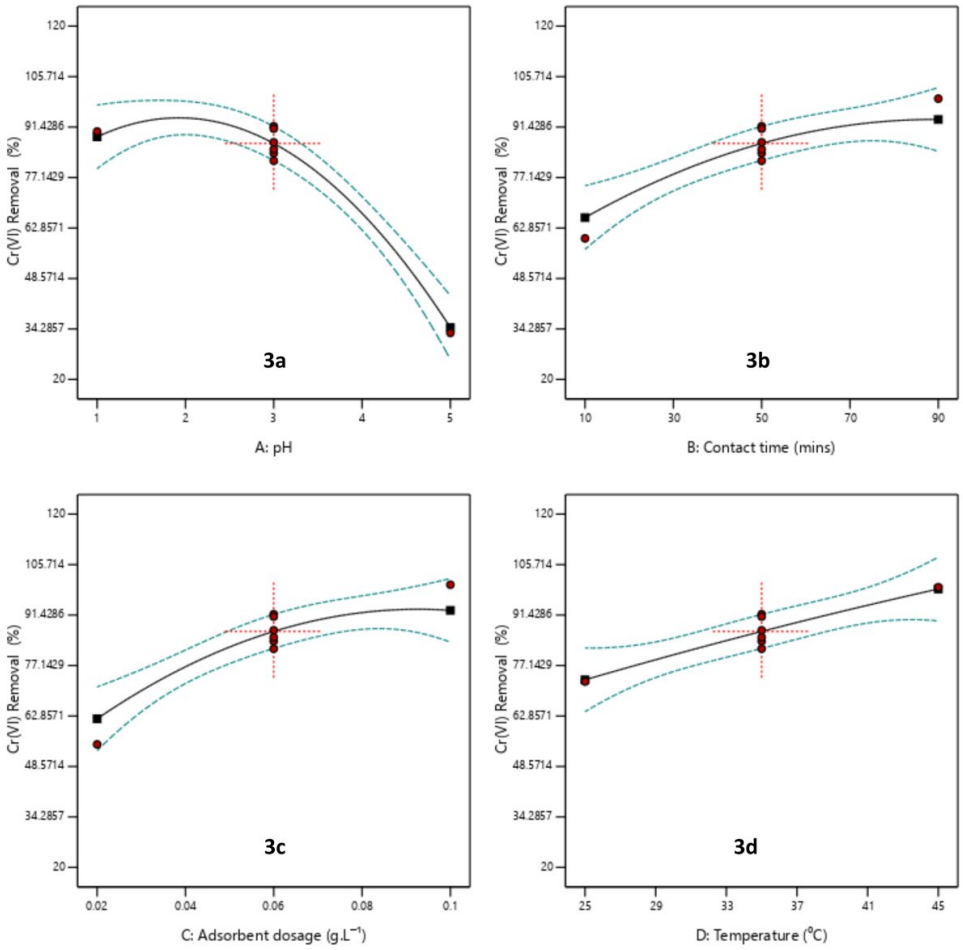

Fig. 3. One factor effects plot for Cr(VI) removal effiency. (a) pH; (b) contact time; (c) adsorbent dosage; and (d) temperature.

The Cr(VI) removal decreased with an increase in pH from 1-5. At pH 2.0, approximately 99% Cr(VI) removal was observed, and this decreases as the pH increases (Figure 3a). The decreased in Cr(VI) adsorption with an increase in pH has also been reported in other studies [47,48]. The pH of the solution affects the speciation of metal ions as well as the surface charge of the adsorbent. The Cr(VI) speciation in aqueous solution is driven by pH. At pH ≤1, Cr(VI) exists primarily as chromic acid (H_2CrO_4). At pH 1-7, the hydrogen chromate ($HCrO_4^-$) ion dominates, whereas above pH 7 only the chromate ion ($CrO4^{-2}$) prevails. The gradual decrease of adsorption from acidic to a neutral pH can be attributed by the gradual conversion of predominantly monovalent hydrogen chromate ($HCrO_4^{-1}$) ions to divalent chromate (CrO_4^{-2}, $Cr_2O_7^{-2}$) ions. This transition occurs because the free energy required for the adsorption of divalent ions is greater than that for monovalent ions, resulting in reduced adsorption of divalent ions on MOBAC [49]. Additionally, as the pH of the surrounding aqueous solution increases, the surface of MOBAC undergoes deprotonation, leading to a decrease in positive surface charges. Consequently, chromate ions with a negative charge experience electrostatic repulsion at higher pH levels, which resulted in decreased adsorption of chromate ions.

The adsorption performance of Cr(VI) were conducted at time intervals 10-90 minutes (Figure 3b). The results revealed that the percent removal of Cr(VI) increases as time proceeds. This might be due to the fast adsorption of Cr(VI) ions on the external surface of the activated carbon at the initial stages [50]. Meanwhile, Figure 3c indicates that with increasing the adsorbent dosage, the removal of Cr(VI) metal ion also increases. It is found that 0.020 g of MOBAC give the lowest adsorption removal which is 54.83 %. As can be seen from Figure 8c, after reaching at 0.100 g of adsorbent dosage, the adsorption process gives a 100% removal of Cr(VI) ions. According to Abdulrasaq & Basiru [51], further increasing the adsorbent dose after reaching its equilibrium state, cannot show significant improvement in removal adsorption. This might be due to the better occupation of lower energy sites in large fractions than the available higher energy sites [52]. Thus, the equilibrium adsorbent dosage for the adsorption of Cr(VI) on activated carbon was found to be around 0.100 g L^{-1}.

A significant increase of Cr(VI) removal was depicted with an increase of temperature from 25°C to 45°C (Figure 3d). An increase in temperature is known to increase the uptake Cr(VI) due to the increase in chemical interaction between the Cr(VI) ions and the activated carbon. It might also be suggested that the Cr(VI) ions were able to overcome the activation energy barrier for adsorption on activated carbon. As a result, the process was endothermic.

Further analysis of the model parameters was performed using three-dimensional response and contour plot. An RSM allows for the investigation of the combined effects of factors on response with the aid of surface plots. In the plots shown in Figure 4, Surface plots were generated by varying two variables at a time, while keeping the others constant at a certain level (usually mid-range). Table 4 lists the significant interactions of the model terms. Out of the six interactions, only three were statistically significant, namely AB, AC, and AD, and response surfaces were generated to study these interactions. As the pH decreases and the contact time increases, the Cr(VI) removal efficiency increases up to 99.47 %. However, it declined when the contact time and pH increased further (Figure 4a). The highest Cr(VI) removal efficiency was obtained at a pH 2 and contact time at 90 minutes.

The Cr(VI) removal efficiency increased up 100%, but it declined when the pH and adsorbent dosage increased further (Figure 4b). Increasing the adsorbent dosage can be attributed to the increased surface area and adsorption sites of adsorbent but no further adsorption could be achieved after reaching its equilibrium state. The highest Cr(VI) removal efficiency was found at medium values of pH 2 and adsorbent dosage of 0.100 g/L. Moreover, increasing the temperature in a lower pH had a positive effect on the Cr(VI) removal. The increased Cr(VI) removal with increasing the temperature may be a result of the faster adsorption of Cr(VI) ions on the external surface of the activated carbon at the initial stages (Figure 4c). The highest Cr(VI) removal efficiency was found at medium values of pH 2 and temperature of 45 °C.

Lastly, the quadratic model equation was optimized to maximize chromium adsorption using mathematical model equations. The overall desirability function, a combination of goals, ranges from zero outside limits to one at the goal. The optimum conditions were achieved by setting the desired goal for Cr(VI) removal efficiency as "maximize" and other independent parameters as “within the range”. Figure 5 shows a ramp desirability made from 30 optimum points via the numerical optimization. By seeking 30 starting points in the response surface changes, the best local maximum was found to be at the pH of 2.16, contact time of 62.7 minutes, adsorbent dosage of 0.065 g L^{-1}, and temperature of 39.8 °C. The model validations have been determined as optimum levels of the process parameters to achieve 99.61% as the maximum percent removal of Cr(VI). The residual Cr(VI) concentration (0.005 mg L^{-1}) at optimized conditions was below the allowable concentrations recommended by the US EPA (0.1 mg L^{-1}) and WHO (0.05 mg L^{-1}).

3.5 Adsorption Isotherms and Kinetics

The adsorption behavior of MOBAC towards Cr(VI) ions were fitted to both Langmuir and Freundlich isotherms in order to verify to whether the interaction between the adsorbent and adsorbate is a chemisorption monolayer adsorption or multilayer adsorption. The linear form of the Langmuir model was obtained by plotting $1/C_e$ against $1/q_e$, while the linear form of the Freundlich isotherm was achieved from the plot of log C_e against log q_e (Fig. 6a and 6b).

The values of the coefficient of determination (R^2) are 0.9908 and 0.9787 (Table 6). It is clear that the correlation coefficients for the Langmuir isotherm is higher than for the Freundlich isotherm, which indicates that the uptake occurs on a homogenous surface by monolayer adsorption and can be described in terms of chemisorption as the formation of an ionic or covalent bonds between the adsorbate and the adsorbent [53]. The essential characteristics of the Langmuir isotherm may also be expressed in terms of a dimensionless separation factor of equilibrium (R_L) which may be calculated from the equation 1 [54].

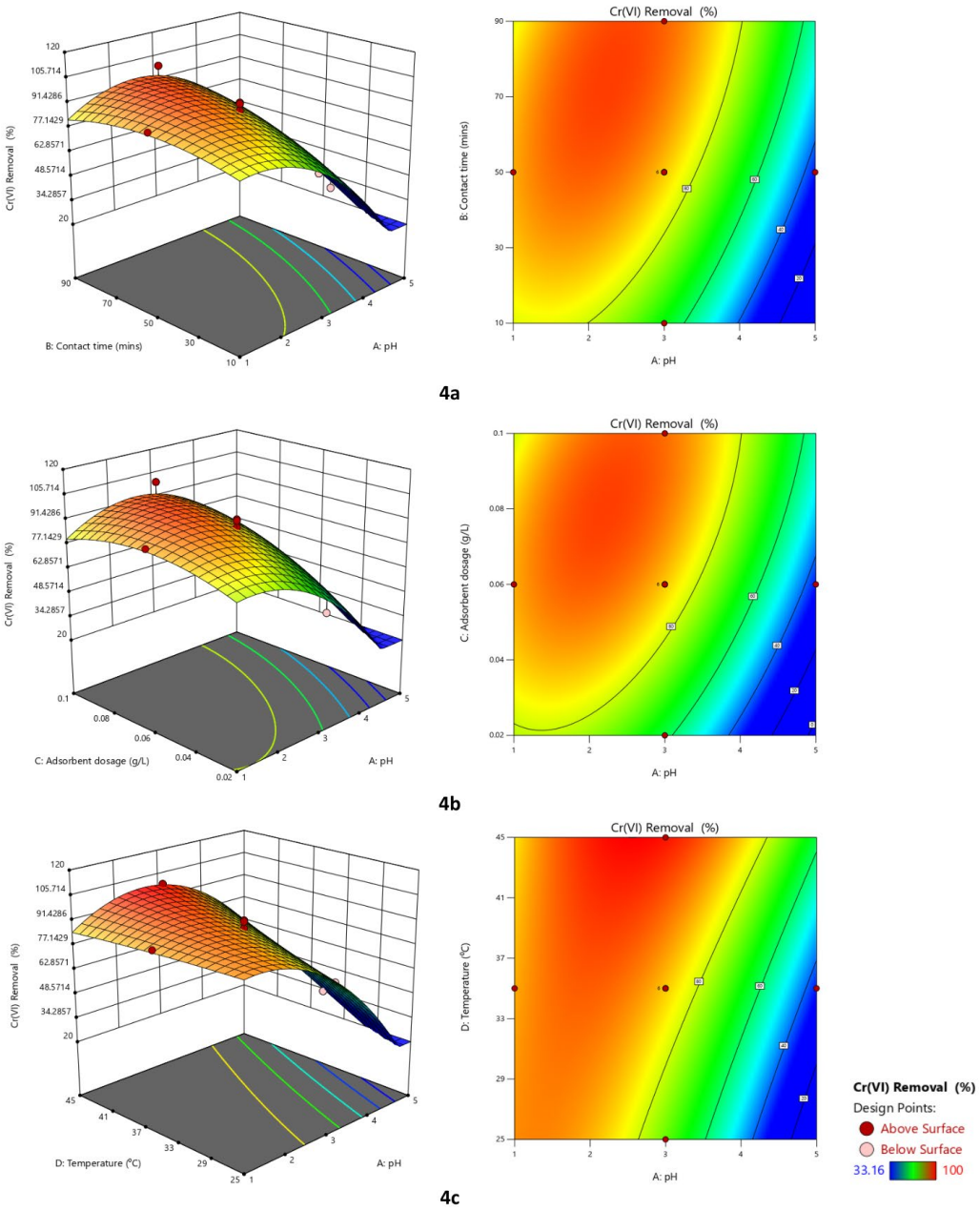

Fig. 4. 3D response plots and contour plots of the Cr(VI) removal efficiences of the optimized MOBAC. (a) pH and contact time; (b) pH and adsorbent dosage; and (c) pH and temperature.

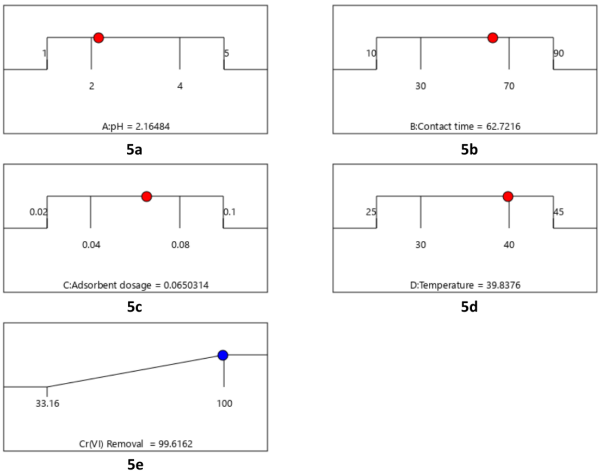

Fig. 5. Desirability ramp for the optimization of the response and variables. (a) pH; (b) contact time; (c) adsorbent dosage; (d) temperature; and (e) Cr(VI) removal.

Table 6. Isotherm Adsorption Parameters of MOBAC towards Cr(VI) ions adsorption.

Isotherm Model	Parameters	
Langmuir	Q_{max} (mg/g)	4.576659
	K_L (mg/L)	5.09324
	R_L (mg/L)	0.115743
	R^2	0.9908
Freundlich	K_F (mg/L)	9.8787
	1/n	0.8019
	R^2	0.9787

The parameter (R_L) is related to the shape of the isotherm

according to the following characteristics: R_L > 1 represent unfavorable adsorption; R_L = 1 corresponds to a linear relationship. 0 < R_L < 1 is favorable adsorption and R_L = 0 is irreversible. In this study, R_L is 0.115 (0 < R_L < 1), which indicates that MOBAC is a good adsorbent for Cr(VI) ion removal.

The investigation of the adsorption kinetics is vital in order to know the rate of the adsorption, which is a good criterion to describe the efficiency of the adsorbent. The data gathered from variation of contact time was used to investigate the kinetic behavior of MOBAC towards the removal of Cr(VI) ions (Table 7). Data were plotted fit to a linearized pseudo-first order and pseudo-second order parameters and the linearized adsorption kinetics respectively (Fig. 6c and 6d).

The R^2 value of the pseudo-second order model (R^2 = 0.9844) was significantly greater than the R^2 value of the pseudo-first order model (R^2 = 0.928), indicating that the pseudo-second order model describes the adsorption kinetic behavior of MOBAC towards Cr(VI) ions. These results conclude that that the interaction between the pollutant and adsorbent at the surface is through chemisorption. Chemisorption involves the interaction of the metal ions (pollutant) and adsorbent via chemical bonding [55]. The results also shows an agreement stated in several other studies including AC obtained from *Mangifera indica* [56]; *Moringa oleifera* bark [33]; bamboo bark [29].

Table 7. Kinetic Adsorption Parameters of MOBAC towards the Adsorption of Cr(VI) ions.

Kinetic Model	Parameters	
Pseudo-First Order	q_1 (mg/g)	0.8898
	K_1 (min^{-1})	5.7 x 10^{-4}
	R^2	0.9280
Pseudo-Second Order	q_2	0.1193
	k_2 (g/mg^{-1} min^{-1})	2.5 x 10^{-4}
	R^2	0.9844

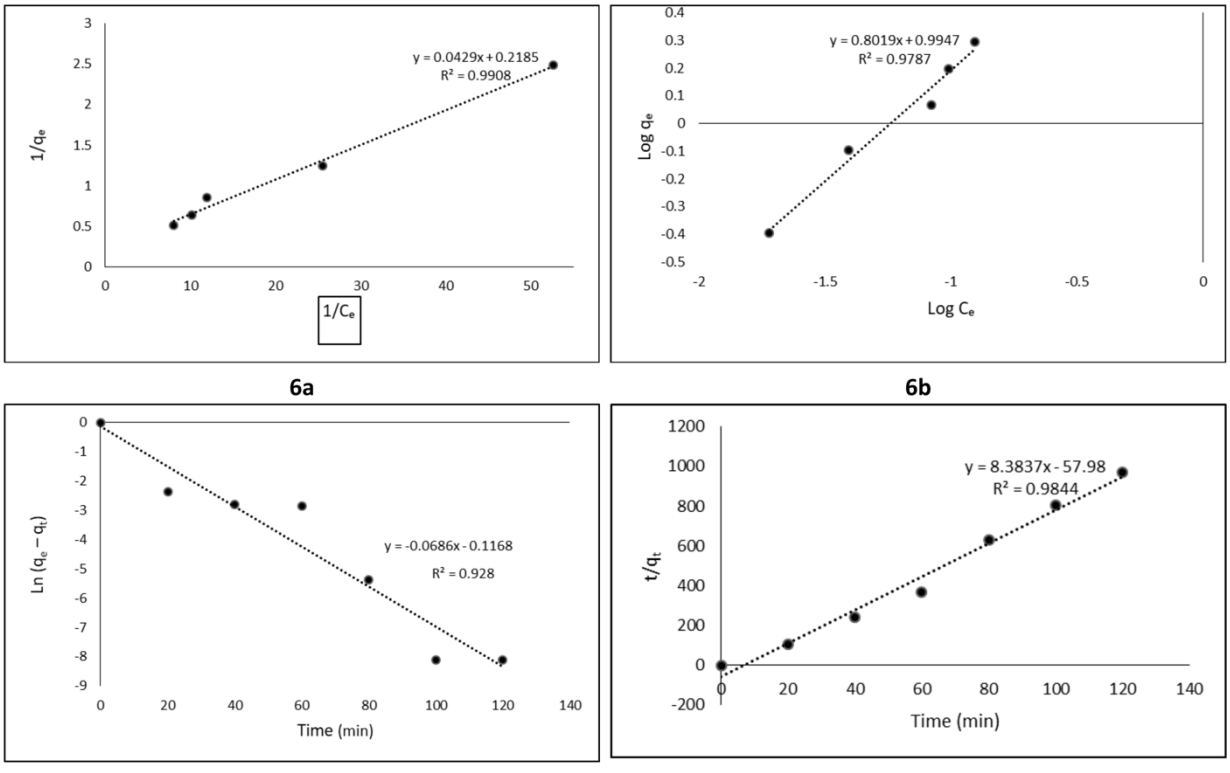

Fig. 6. Adsorption isotherms and kinetics for Cr(VI) adsorption by MOBAC. (a) Langmuir adsorption isotherm; (b) Freundlich adsorption isotherm; (c) Pseudo-First order kinetics; and (d) Pseudo-Second order kinetics.

The performance of MOBAC developed in the current study was compared with other adsorbent for the removal of Cr(VI) ions. Adebayo et al. [31] found out the adsorption capacities of goethite (G), activated carbon (AC) and their composite (GAC) for Cr(VI) are 6.627, 5.455 and 6.354 mg g^{-1} with 0.02 g adsorbent within contact time of 60, 180 and 30 min for G, AC and GAC, respectively at optimum pH of 3. Kobya [27] reported in his study that the adsorption capacity of Hazelnut shell activated carbon as calculated from the Langmuir isotherm was 170 mg g^{-1} at an initial pH of 1.0 for a Cr(VI) solution of 1000 mg L^{-1} concentration. Another study by Doke & Khan [28] revealed that wood apple shell activated carbon achieved a maximum adsorption capacity of 151.51 mg g^{-1} with 1.25 g L^{-1} of adsorbent at an initial concentration of 75 mg L^{-1} for Cr(VI) ion adsorption. Comparing these adsorbents, it is evident that MOBAC showed promising potential for Cr(VI) ion removal from aqueous systems. With a minimal amount of MOBAC (0.065 g L^{-1}), 99.612 % of Cr(VI) ions are removed from aqueous solution.

4. Conclusions

The present study reports the performance of MOBAC in Cr(VI) metal removal from aqueous solution using RSM with CCD statistical analysis. The influence of operational

parameters such as the solution pH, contact time, adsorbent dosage, and temperature was considered. The results revealed that the developed RSM quadratic model could be successfully applied for optimizing the process variables and interactions in the response. At this optimum condition, the residual concentration (0.005 mg L^{-1}) of Cr(VI) considered is within the maximum limit recommended by the US EPA (0.1 mg L^{-1}) and WHO (0.05 mg L^{-1}). However, further investigations may be conducted to it is recommended to provide comprehensive analyses on the effectiveness of MOBAC, to wit: (1) perform Raman scattering measurements to further investigate Cr-O bonding and hydrogen bonding with water; (2) use MOBAC as an adsorbent for different types of contaminants; (3) additional conditions should be considered such as point of zero charge of the adsorbent, effect of mixing speed, thermodynamics study to further understand the adsorption behavior of MOBAC; and (4) desorption process must also be conducted to verify how many times MOBAC can be reused. Nevertheless, the results of the present study suggest that the use of MOBAC can be a good alternative for the current expensive methods of removing the Cr(VI) ions from aqueous solution.

Acknowledgments

The authors express their gratitude to N.J.B. Agosto, G.D. Leopoldo, M.K.B. Carmona, and F.N.P. Hamoy for their scholarly inputs throughout the conduct of the study. Moreover, the authors extend their heartfelt thanks to the anonymous reviewers for their constructive feedback that greatly contributed to the finality of this manuscript.

Author Contributions

Conceptualization, E.P.A., D.P.A., N.F.A.A.; Methodology, E.P.A., N.F.A.A; Investigation and Formal Analysis, E.P.A., D.P.A.; Software, E.P.A.; Resources, E.P.A., D.P.A.; Supervision, N.F.A.A.; Validation, E.P.A., N.F.A.A.; Visualization, E.P.A., D.P.A.; Writing – Original Draft, D.P.A.; Writing – Review and Editing, E.P.A., D.P.A., N.F.A.A. All authors have read and agreed to the published version of the manuscript.

References and Notes

[1] Mustafa, H. M.; Hayder, G. *Ain Shams Eng. J.* **2020**, *12*, 355. [Crossref]

[2] Safauldeen, S. H.; AbuHasan, H.; Abdullah, S. R. S. *J. Ecol. Eng.* **2019**, *20*, 177. [Crossref]

[3] Renge, V. C.; Khedkar, S. V.; Pandey Shraddha, V. *Sci. Rev. Chem. Commun.* **2012**, *2*, 580.

[4] Chang, L. W. Toxicology of Metals. *Lewis Publishers*, Boca Raton, 1996, p. 1052.

[5] Babula, P.; Adam, V.; Opatrilova, R.; Zehnalek, J.; Havel, L.; Kizek, R. *Environ. Chem. Lett.* **2008**, *6*, 189. [Crossref]

[6] Cabtingan, L. K.; Agapay, R. C.; Rakels, J. L. L.; Ottens, M.; Van Der Wielen, L. A. M. *Ind. Eng. Chem. Res.* **2001**, *40*, 2302. [Crossref]

[7] Srinath, T.; Verma, T.; Ramteke, P. W.; Garg, S. K. *Chemosphere* **2002**, *48*, 427. [Crossref]

[8] Aravindhan, R.; Madhan, B.; Rao J. R.; Nair, B. U.; Ramasami, T. *Environ. Sci. Technol.* **2004b**, *38*, 300. [Crossref]

[9] Deng, S.; Ting, Y. P.; Yu, G. *Water Sci. Technol*. **2006**, *54*, 1. [Crossref]

[10] Krishnani, K. K.; Srinives, S.; Mohapatra, B. C.; Boddu, V. M.; Hao, J., Meng, X., et al. *J. Hazard. Mater*. **2013**, *252*, 99. [Crossref]

[11] Kera, N. H.; Bhaumik, M.; Pillay, K.; Ray, S. S.; Maity, A. *J. Colloid Interf. Sci*. **2017**, *503*, 214. [Crossref]

[12] Wang, B.; Wu, T.; Angaiah, S.; Murugadoss, V.; Ryu, J.E.; Wujcik, E.K.; Lu, N.; Young, D.P.; Gao, Q.; Guo, Z. *ES Materials & Manufacturing* **2018**, *2*, 35. [Crossref]

[13] Niu, J.; Ding, P.; Jia, X.; Hu, G.; Li, Z. *Sci. Total Environ.* **2019**, *688*, 994. [Crossref]

[14] Zarringhalam, M.; Ahmadi-Danesh-Ashtiani, H.; Toghraie, D.; Fazaeli, R. *J. Mol. Liquids* **2019**, *293*, 111474. [Crossref]

[15] Ou, B.; Wang, J.; Wu, Y.; Zhao, S.; Wang, Z. *Chem. Eng. J.* **2020**, *380*, 122600. [Crossref]

[16] Reck, I. M.; Paixao, R. M.; Bergamasco, R.; Vieira, M. F.; Vieira, A. M. S. *J. Clean. Prod*. **2018**, *171*, 85. [Crossref]

[17] Bhattacharjee, C.; Dutta, S.; Saxena, V. *Environmental Advances*. **2020**, *2*, 100007. [Crossref]

[18] Gupta, V. K.; Rastogi, A. *J. Hazard. Mater*. **2009**, *163*, 396. [Crossref]

[19] Kyzas, G. Z.; Kostoglou, M. *Materials* **2014**, *7*, 333. [Crossref]

[20] Masekela, D.; Yusuf, T. L.; Hintsho-Mbita, N. C.; Mabuba, N. *Front. Water* **2022**, *4*, 722269. [Crossref]

[21] Anastopoulos, I.; Pashalidis, I.; Orfanos, A. G.; Manariotis, I. D.; Tatarchuk, T.; Sellaoui L.; Bonilla-Petriciolet A.; Mittal A.; Núñez-Delgado A. *J. Environ. Manag*. **2020**, *261*, 110236. [Crossref]

[22] Sadh, P. K.; Duhan, S.; Duhan, J. S. *Bioresour. Bioprocess* **2018**, *5*, 1. [Crossref]

[23] Leimkuehler, E. P. Production, Characterization, and Applications of Activated Carbon. University of Missouri. **2010**.

[24] Ko, D. C. K.; Mui, E. L. K.; Lau, K. S. T.; McKay, G. *Waste Manag*. **2004**, 24, 875. [Crossref]

[25] Cimino, G.; Passerini, A.; Toscano, G. *Water Res*. **2000**, *34*, 2955. [Crossref]

[26] Demirbas, E. *Adsorpt. Sci. Technol*. **2003**, *21*, 951. [Crossref]

[27] Kobya, M. *Adsorpt. Sci. Technol.* **2004**, *22*, 51. [Crossref]

[28] Doke, K. M.; Khan, E. M. *Arab. J. Chem.* **2012**, *10*, S252. [Crossref]

[29] Zhang, Yan-Juan; Ou, Jie-Lian; Duan, Zheng-Kang; Xing, Zhen-Jiao; Wang, Yin. *Colloids Surf., A* **2015**, *481*, 108. [Crossref]

[30] Alvarez-Galvan, Y.; Minofar, B.; Futera, Z.; Francoeur, M.; Jean-Marius, C.; Brehm, N.; Yacou, C.; Jauregui-Haza, U.J.; Gaspard, S. *Molecules* **2022**, *27*, 6040. [Crossref]

[31] Adebayo, G. B.; Adegoke, H. I.; Fauzeeyat, S. *Appl. Water Sci.* **2020,** *10*, 213. [Crossref]

[32] Ali, H.; Khan, E. *Hum. Ecol. Risk Assess. Int. J*. **2019**, *25*, 1353. [Crossref]

[33] Azad, S.; Hassan, M. S.; Shahinuzzaman, M.; Azhari, S. *Int. J. Eng. Res. Technol.* **2020**, *9*, 695. [Crossref]

[34] Acharya, J.; Sahu, J. N.; Sahoo, B. K.; Mohanty C. R.;

Meikap, B. C. *Chem Eng J*. **2009**, *150*, 25. [Crossref]

[35] Saikaew, W.; Kaewsarn, P.; Saikaew, W. International Journal of Chemical, Molecular, Nuclear, Materials and Metallurgical Engineering. **2009**, *3*, 393.

[36] Demirbas, E. *J. Hazard Mater*. **2008**, 157, 220. [Crossref]

[37] Abdullah, N. S.; Hussin, M. H.; Sharifuddin, S. S.; Yusoff, M. A. M. *National Hydraulic Research Institute of Malaysia* **2017**, *29*, 7.

[38] Kalavathy, M. H.; Miranda, L. R. *Chem. Eng. J.* **2010**, *158*, 188. [Crossref]

[39] Langmuir, I. *J. Am. Chem. Soc*. **1916**, *38*, 2221. [Crossref]

[40] Dada, A. O.; Olalekan, A. P.; Olatunya, A. M.; Dada, O. J. I. J.C. *IOSR J. Appl. Chem*. **2012**, *3*, 38. [Crossref]

[41] Duranoglu, D.; Trochimczuk, A. W.; Beker, U. *Chem. Eng. J*. **2012**, *187*, 193. [Crossref]

[42] Lagergren, S. *Handlingar* **1898**, *24*, 1.

[43] Batista, A. C.; Villanueva, E. R.; Amorim, R. V. S. et al. *Molecules* **2011**, *16*, 3569. [Crossref]

[44] Pérez Marín, A. B.; Aguilar, M. I.; Ortuño, J. F.; Meseguer, V. F.; Sáez, J.; Lloréns, M. *J. Chem. Technol. Biotechnol.* **2010**, *85*, 1310. [Crossref]

[45] Hamadi, N. K.; Chen, X. D.; Farid, M. M; Lu, M. G. Q. *Chem. Eng. J*. **2001**, *84,* 95. [Crossref]

[46] Bashir, M. J. K.; Amr, S. A.; Aziz, Q.; Ng, C. A. *Middle East J. Sci. Res.* **2015**, *23*, 244. [Link]

[47] Fito, J.; Tibebu, S.; Nkambule, T. T. I. *BMC Chemistry* **2023**, *17*, *4*. [Crossref]

[48] Yan, Bz., Chen, Zf. *Appl Water Sci*. **2019**, *9*, 61. [Crossref]

[49] Adapa, S.; Malani, A. *Sci. Rep*. **2018**, *8*, 12198. [Crossref]

[50] Gorzin, F.; Abadi, M. M. B. R. *Ads Sci Techn*. **2018**, 36, 149. [Crossref]

[51] Abdulrasaq, O. O.; Basiru, O. G. *Afr. J. Environ. Sci. Technol.* **2010**, *4*, 7. [Crossref]

[52] Shakya, A.; Agarwal, T. *J. Mol. Liq*. **2019**, *293*, 111497. [Crossref]

[53] Dhar Das, D.; Pradhan. J.; Nath Das, S.; Thakur, R. S. *J. Colloid 2 Int. Sci*. **2000**, *232*, 235. [Crossref]

[54] Badu, B. V.; Gupta, S. *Adsorption* **2008**, *14*, 85. [Crossref]

[55] Wan, M. W.; Kan, C. C.; Rogel, B. D.; Dalida, M. L. P. *Carbohyd. Polym*. **2010**, *80*, 891. [Crossref]

[56] Duraisamy, R.; Mechoro, M.; Seda, T.; Khan, M. A. *Cogent Engineering* **2020**, *7*, 1. [Crossref]

How to cite this article

Acut, E. P.; Anorico, N. F. A.; Acut, D. P. *Orbital: Electron. J. Chem.* **2023**, *15*, 186. DOI: http://dx.doi.org/10.17807/orbital